Emerald Insight

Rapid Prototyping Journal

Efficient volumetric error compensation technique for additive manufacturing machines
Carlos Cajal Jorge Santolaria David Samper Jesus Velazquez

Article information:

To cite this document:
Carlos Cajal Jorge Santolaria David Samper Jesus Velazquez , (2016),"Efficient volumetric error compensation technique for additive manufacturing machines", Rapid Prototyping Journal, Vol. 22 Iss 1 pp. 2 - 19
Permanent link to this document:
http://dx.doi.org/10.1108/RPJ-05-2014-0061

Downloaded on: 09 February 2016, At: 23:54 (PT)
References: this document contains references to 34 other documents.
To copy this document: permissions@emeraldinsight.com
The fulltext of this document has been downloaded 112 times since 2016*

Users who downloaded this article also downloaded:

Marlon Wesley Machado Cunico, Jonas de Carvalho, (2016),"Development of novel additive manufacturing technology: an investigation of a selective composite formation process", Rapid Prototyping Journal, Vol. 22 Iss 1 pp. 51-66 http://dx.doi.org/10.1108/RPJ-04-2014-0049

David Joguet, Sophie Costil, Hanlin Liao, Yoann Danlos, (2016),"Porosity content control of CoCrMo and titanium parts by Taguchi method applied to selective laser melting process parameter", Rapid Prototyping Journal, Vol. 22 Iss 1 pp. 20-30 http://dx.doi.org/10.1108/RPJ-09-2013-0092

Maria Doubenskaia, Sergey Grigoriev, Ivan Zhirnov, Igor Smurov, (2016),"Parametric analysis of SLM using comprehensive optical monitoring", Rapid Prototyping Journal, Vol. 22 Iss 1 pp. 40-50 http://dx.doi.org/10.1108/RPJ-04-2014-0046

RMIT UNIVERSITY

Access to this document was granted through an Emerald subscription provided by emerald-srm:393177 []

For Authors

If you would like to write for this, or any other Emerald publication, then please use our Emerald for Authors service information about how to choose which publication to write for and submission guidelines are available for all. Please visit www.emeraldinsight.com/authors for more information.

About Emerald www.emeraldinsight.com

Emerald is a global publisher linking research and practice to the benefit of society. The company manages a portfolio of more than 290 journals and over 2,350 books and book series volumes, as well as providing an extensive range of online products and additional customer resources and services.

Emerald is both COUNTER 4 and TRANSFER compliant. The organization is a partner of the Committee on Publication Ethics (COPE) and also works with Portico and the LOCKSS initiative for digital archive preservation.

*Related content and download information correct at time of download.

Downloaded by RMIT University At 23:54 09 February 2016 (PT)

Efficient volumetric error compensation technique for additive manufacturing machines

Carlos Cajal
Quality, Centro Universitario de la Defensa, University of Zaragoza, Zaragoza, Spain, and
Jorge Santolaria, David Samper and Jesus Velazquez
Design and Manufacturing Engineering Department, University of Zaragoza, Zaragoza, Spain

Abstract

Purpose – This paper aims to present a methodology for volumetric error compensation. This technique is applied to an Objet Eden350V 3D printer and involves a custom measurement strategy.

Design/methodology/approach – The kinematic model of the printer is explained, and its error model is simplified to 18 independent error functions. Each error function is defined by a cubic Legendre polynomial. The coefficients of the polynomials are obtained through a Levenberg–Marquardt optimization process. This optimization process compares, in an iterative algorithm, nominal coordinates with actual values of the cloud of points. The points are built in the faces of a gauge artefact as conical sockets defining one unique point for each socket. These points are measured by a coordinate measuring machine self-centring measurement process.

Findings – Most of the errors of the 3D printer are systematic. It is possible to obtain an improvement of 70 per cent in terms of global mean error reduction in single points within a volume of 120 × 120 × 40 mm. The forecast of the final error compensation fully matches the actual final error.

Practical implications – This methodology can be used for accuracy improvement in additive manufacturing machines.

Originality/value – Unlike the calculation of geometric errors, the proposed parametric determination through optimization of the error model allows global error reduction, which decreases all sort of systematic errors concurrently. The proposed measurement strategy allows high reliability, high speed and operator independence in the measurement process, which increases efficiency and reduces the cost. The proposed methodology is easily translated to other rapid prototyping machines and allows scalability when replicating artefacts covering any working volume.

Keywords Optimization techniques, Additive manufacturing, Measurement, Accuracy, Volumetric error compensation, 3D printer, Coordinate measuring machine

Paper type Research paper

Downloaded by RMIT University At 23:54 09 February 2016 (PT)

1. Introduction

In recent years, an increasing number of rapid prototyping (RP) technologies have emerged. As prices decrease, these machines are spreading from prototyping to actual end-user manufacturing (Campbell *et al.*, 2012). Therefore, it must be ensured that quality requirements regarding dimensional and geometrical accuracy are met for final products. Additive manufacturing (AM) machines have several advantages, but accuracy is not among them (Dimitrov *et al.*, 2006). In that direction, many studies have aimed to clarify whether RP technologies, AM in particular, are suitable for final product production from a dimensional accuracy point of view (Liu *et al.*, 1998a, 1998b; Choi *et al.*, 2002; Hanumaiah and Ravi, 2007; Xu *et al.*, 2000; Moylan *et al.*, 2012).

Various factors are responsible for the traditional lack of accuracy in AM technologies. According to (Yan and Gu, 1996), a distinction should be made between mathematical error, process-related error and material-related error depending on the nature of the error source. The combination of all of them is responsible for the final dimensional quality of the manufactured workpiece independently of the process phase that causes them (CAD modelling, data preparation, layer construction and post-processing). The improvement of this dimensional quality, to bring the performance of traditional manufacturing to AM, is the main goal of this paper. Therefore for that purpose, traditional accuracy improvement techniques could result very useful.

Research on accuracy improvement profits from a long tradition in classical manufacturing technologies like machine tooling and even more in the case of measurement machines (Sartori and Zhang, 1995; Zhu *et al.*, 2010). Despite the discrepancies, AM and traditional machining share many of the typical error sources of machine tools, which are categorized as kinematic errors, thermo-mechanical errors, loads, dynamic forces, motion control and control software. Thus, they can also share the available improvement techniques. There are two approaches to improving a manufacturing machine: improvement of the machine design or modification of the operation parameters to indirectly improve the resulting parts. Internal

The current issue and full text archive of this journal is available on Emerald Insight at: **www.emeraldinsight.com/1355-2546.htm**

Rapid Prototyping Journal
22/1 (2016) 2–19
© Emerald Group Publishing Limited [ISSN 1355-2546]
[DOI 10.1108/RPJ-05-2014-0061]

Received 19 October 2013
Revised 7 May 2014
20 June 2014
Accepted 20 August 2014

Downloaded by RMIT University At 23:54 09 February 2016 (PT)

operation parameters are restricted to manufacturers. The same applies to constructive modifications. Nevertheless, input modification, also known as software compensation, has been proven to be effective in all sort of machines without machine alteration (Tong *et al.*, 2004; Wang *et al.*, 2002; Jung *et al.*, 2006).

Compensation techniques predict the error committed by the machine and consequently modify the target in the opposite direction, improving workpiece accuracy. Some requirements must be met to ensure the viability of these techniques (Sartori and Zhang, 1995) and, accordingly, each of them is discussed in the various sections of this paper:

- Systematic error components must be significantly greater than random errors that are not subject to compensation.
- Proper error modelling is mandatory. Measurement errors are interpreted as machine errors and therefore inadequate measurement effects can modify error functions, giving incorrect compensations.
- Error measurements and error compensations must be made with reference to the machine-embedded absolute coordinate system.
- Short-period errors cannot be compensated and this can be a problem for scale errors like subdivision errors depending on the mechanical components of the machine.
- The thermal conditions of the machine are a concern in compensation techniques because they are likely to be the most important limitation.
- The real-time compensation process must not decrease machine performance.

Based on the above information, there are some aspects that make AM technologies the top target of software compensation techniques:

- Not only fabrication process errors but also data preparation errors can be of a systematic nature. As the combined effect of systematic errors is compensated concurrently, whether or not they come from data preparation, constructive geometrical defects, thermal expansion or tool wear becomes irrelevant.
- The STL (STereoLithography) file format, which is the *de facto* standard in additive manufacturing, allows easy manipulation to incorporate compensation. The same applies to the SLC (SLiCe) file format.
- Although most of the additive processes are exothermic, when the thermal reaction is steady in the process it can be considered as a systematic effect, in contrast to cutting friction and active liquid refrigeration in chip removal processes.
- Perhaps the most significant cause of systematic prevalence that applies to some AM technologies is the single path. The addition tool always performs the same route with the same orientation and speed to reach certain coordinates in the working volume. This fact is rare in other manufacturing processes like milling; however, it has been observed in the Objet Eden350V, whose potential improvement seems great.

In this paper, the lack of accuracy is addressed using software compensation techniques for an Objet 350V 3D printer. First of all, as its name indicates, random error sources can never be compensated. Therefore, the scope of the systematic error has to be determined. This is achieved by building and measuring some gauge workpieces to compare actual measurements with the ideal dimensions. The ultimate goal is to increase the performance of the machine through computer-assisted design (CAD) data manipulation, so error volumetric model optimization seems to be the best approach. The gauge workpiece measurement results make it possible to determine the coefficients of the error functions that best fit the kinematic error model of a ZFXY machine, such as the Objet Eden350V, used in this research. The 18 geometric errors, in which the error model of the machine (Wilhelm *et al.*, 1997) can be decomposed, are represented by cubic Legendre polynomial functions. The coefficients of each of these error polynomials are identified by a Levenberg-Marquardt (L-M) optimization algorithm (Levenberg, 1944; Marquardt, 1963).

Volumetric techniques require a high density of data points in the working volume (Aguado *et al.*, 2012a, 2012b). This is complicated to achieve with reference spheres; however, the use of conical sockets to measure single points solves the problem. Instead of probing several points to calculate the centre of a reference sphere, one single probing provides the socket centre coordinates. On the other hand, the use of high-precision measurement instruments such as coordinate measuring machines (CMMs) implies a high cost in terms of time and materials. Although this is an important concern, it is not the only one. The CMM is not immune to the operator being an additional source of error (Schwenke *et al.*, 2008). Accordingly, an automatic measurement methodology that has high reliability and low cost in terms of time consumption, thanks to self-centring probing and conical sockets, has been carried out.

The discrete error values calculated from the polynomials, obtained in an iterative optimization process, show the final achievable accuracy, which is fundamental in the manufacturing technology or machine selection process. This theoretical improvement must be compared with actual results, first with conical socket gauge artefacts and later with actual geometries.

2. Kinematic model

In the study by Jung *et al.*, 2006, three basic phases of compensation methods were established:

1. kinematic modelling from the constructive characteristic of the machine;
2. parametric determination of each of the composing errors of the machine. This can be done directly or indirectly; and
3. compensation from the forecasted error model.

A multi-axis machine's kinematic chains can be represented, schematically, by a succession of linear and rotational displacements of its various elements (Hocken *et al.*, 1977). The basic elements that make up the kinematic chain of a linear-axis machine are the bedplate, the linear axes, the tool and the workpiece. These machines can be categorized depending on the distribution of the movable axis relative to the bedplate. There will be always two kinematic chains from the machine bed to the tip of the tool, addition device, or, in the case, of AM printers, the printhead. So the denomination of the machine depends on the configuration of the two chains. The machine bedplate is represented by the letter F and the different linear axes by the letters X, Y and Z depending on which coordinate is moved by each guide (Figure 1).

The letters before F represent the possible movements of the workpiece with respect to the bedplate, and the letters after F

Figure 1 Reference system and movements

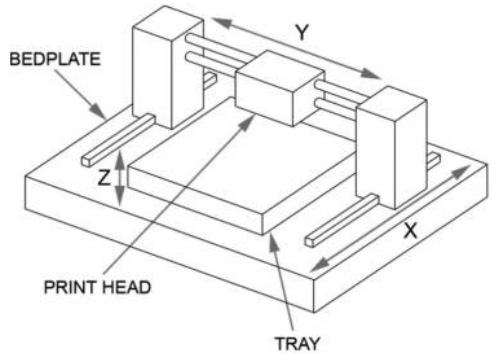

indicate the possible movement of the tool relative to the bedplate. In the case of the Objet350V 3D printer, the X and Y guides move the printhead and the piece is on a tray that controls the Z axis. Therefore, it is considered a ZFXY three-linear-axes machine.

The kinematic model of the printer can be seen in Figure 2, where X [equation (6)], Y [equation (8)] and Z [equation (2)] are vectors which represent the nominal displacements and the linear errors of the printer displacement guides; W [equation (4)] is a vector whose elements are the offset linking the Z guide and the contact point between the printhead and the workpiece through the workpiece; and finally T [eqiation (10)] is a vector representing the offset linking the Y guide with the contact point between the printhead and the workpiece through the printhead.

The kinematic chain (KC_1) that goes from the bed plate to the printhead through the workpiece (Figure 2) can be written mathematically using two translation vectors $\vec{Z}$ and $\vec{W}$ and an infinitesimal rotation matrix $\vec{R}_Z^{-1}$:

$$KC_2 = \vec{Z} + \vec{R}_Z^{-1} \cdot \vec{W} \tag{1}$$

$$\vec{Z} = \begin{pmatrix} EXZ - z \cdot EBO \\ EYZ - z \cdot EAO \\ z + EZZ \end{pmatrix} \tag{2}$$

In all cases, x, y and z are the nominal displacement across the X, Y and Z guides, while the correspondence of *EXZ*, *EYZ*, *EZZ*, *EAO* and *EBO* is shown in Table I.

Figure 2 Vector diagram of the kinematic chains

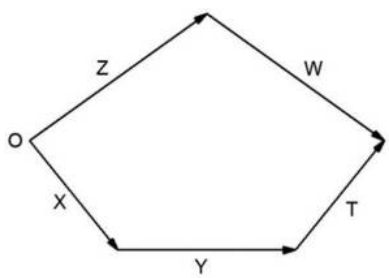

Table I Twenty-one errors according to UNE-ISO 230

X-axis		Y-axis		Z-axis	
EXX	**Position**	**EYY**	**Position**	**EZZ**	**Position**
EXY	Straightness	EYX	Straightness	EZX	Straightness
EXZ	Straightness	EYZ	Straightness	EZY	Straightness
EAX	Roll	EAY	Pitch	EAZ	Pitch
EBX	Pitch	EBY	Roll	EBZ	Yaw
ECX	Yaw	ECY	Yaw	ECZ	Roll
EAO	Squareness	EBO	Squareness	ECO	Squareness

In a kinematic chain, the displacements of an element are affected by the rotation error of the elements that are placed before it, and therefore the translation vector $\vec{W}$ is multiplied by the inverse of the infinitesimal rotation matrix $\vec{R}_Z^{-1}$ [equation (3)]:

$$\vec{R}_Z^{-1} = \begin{pmatrix} 1 & -ECZ & EBZ \\ ECZ & 1 & -EAZ \\ -EBZ & EAZ & 1 \end{pmatrix} \tag{3}$$

Definitions of *EAZ*, *EBZ* and *ECZ* are shown in Table I.

$$\vec{W} = \begin{pmatrix} X_p \\ Y_p \\ Z_p \end{pmatrix} \tag{4}$$

The X–Y–T kinematic chain (KC_2) can be mathematically expressed as shown in equations (5-10):

$$KC_2 = \vec{X} + \vec{R}_X^{-1} \cdot \vec{Y} + \vec{R}_X^{-1} \cdot \vec{R}_Y^{-1} \cdot \vec{T} \tag{5}$$

$$\vec{X} = \begin{pmatrix} x + EXX \\ EYX \\ EZX \end{pmatrix} \tag{6}$$

Definitions of *EXX*, *EYX* and *EZX* are also shown in Table I.

The translation vector $\vec{Y}$ is affected by the infinitesimal rotation matrix [equation (7)]:

$$\vec{R}_X^{-1} = \begin{pmatrix} 1 & -ECX & EBX \\ ECX & 1 & -EAX \\ -EBX & EAX & 1 \end{pmatrix} \tag{7}$$

EAX, *EBX* and *ECX* are defined in Table I.

The value of translation vector $\vec{Y}$ is given by equation (8):

$$\vec{Y} = \begin{pmatrix} EXY - y \cdot ECO \\ y + EYY \\ EZY \end{pmatrix} \tag{8}$$

EXY, *EYY*, *EZY* and *ECO* are defined in Table I.

Vector $\vec{T}$ is affected by the two infinitesimal rotation matrices linked to the two preceding vectors, $\vec{R}_X^{-1}$ equation (7) and $\vec{R}_Y^{-1}$ equation (9):

$$\vec{R}_Y^{-1} = \begin{pmatrix} 1 & -ECY & EBY \\ ECY & 1 & -EAY \\ -EBY & EAY & 1 \end{pmatrix} \tag{9}$$

EAY, *EBY* and *ECY* are defined in Table I.

Downloaded by RMIT University At 23:54 09 February 2016 (PT)

Downloaded by RMIT University At 23:54 09 February 2016 (PT)

Vector $\vec{T}$ is defined in equation (10), where x_t, y_t and z_t are the dimensions of the tool offset:

$$T = \begin{pmatrix} x_t \\ y_t \\ z_t \end{pmatrix} \quad (10)$$

Both kinematic chains share their initial and final points: the bedplate as the initial one and the contact point between the printer head and the workpiece as the final one. The printer kinematic model can be written as shown in equation (11):

$$\vec{Z} + \vec{R}_Z^{-1} \cdot \vec{W} = \vec{X} + \vec{R}_X^{-1} \cdot \vec{Y} + \vec{R}_X^{-1} \cdot \vec{R}_Y^{-1} \cdot \vec{T} \quad (11)$$

The rotation matrix $\vec{R}_Z$ [equation (12)] can be expressed as:

$$\vec{R}_Z = \begin{pmatrix} 1 & ECZ & -EBZ \\ -ECZ & 1 & EAZ \\ EBZ & -EAZ & 1 \end{pmatrix} \quad (12)$$

Solving $\vec{W}$ leaves equation (13 and 14):

$$\vec{W} = \vec{R}_Z\left(\vec{X} + \vec{R}_X^{-1} \cdot \vec{Y} + \vec{R}_X^{-1} \cdot \vec{R}_Y^{-1} \cdot \vec{T} - \vec{Z}\right) \quad (13)$$

$$\vec{W} = \vec{R}_Z \cdot \vec{X} + \vec{R}_Z \cdot \vec{R}_X^{-1} \cdot \vec{Y} + \vec{R}_Z \cdot \vec{R}_X^{-1} \cdot \vec{R}_Y^{-1} \cdot \vec{T} - \vec{R}_Z \cdot \vec{Z} \quad (14)$$

Operating the equations, the values of X_p, Y_p and Z_p are obtained.

X_p represents the actual value of the X coordinate as a function of the nominal values, and the same applies to Y_p and Z_p. These coordinates are defined in the machine reference system (MRS). Equations (15-17) define the actual values of the coordinates as a function of the nominal values, the dimensions of the tool offset and the 21 errors of the kinematic model (Table I):

$$X_p = x + [EXX + EXY - EXZ] - y[ECO + ECX - ECZ] + z[EBO + EBZ] + x_t - y_t[ECX + ECY - ECZ] + z_t[EBX + EBY - EBZ] \quad (15)$$

$$Y_p = y + [EYX + EYY - EYZ] - x \cdot ECZ + z[EAO - EAZ] + x_t[ECX + ECY - ECZ] + y_t - z_t[EAX + EAY - EAZ] \quad (16)$$

$$Z_p = -z + [EZX + EZY - EZZ] + x \cdot EBZ + y[EAX - EAZ] - x_t[EBX + EBY - EBZ] + y_t[EAX + EAY - EAZ] + z_t \quad (17)$$

The dimensions of the tool offset (x_t, y_t, z_t) are null, considering that the Y-axis is at the contact point of the printhead with the workpiece. Additionally, as explained above assimilating the axes' squareness errors to straightness (Kruth *et al.*, 1994), the following equations result:

$$X_p = x + [EXX + EXY - EXZ] - y \cdot [ECX - ECZ] + z \cdot EBZ \quad (18)$$

$$Y_p = y + [EYX + EYY - EYZ] - x \cdot ECZ - z \cdot EAZ \quad (19)$$

$$Z_p = -z + [EZX + EZY - EZZ] + x \cdot EBZ + y[EAX - EAZ] \quad (20)$$

In the study by Sartori and Zhang, 1995, it is stated that the machine must have an embedded absolute reference system, named as MRS. Therefore, error measurements and error compensations must be done with reference to this coordinate system. As each workpiece is measured according to its self-defined local reference system, named as part reference system (PRS), a mechanism to relate the two reference systems has to be put in place.

As shown in Figure 3, M_1 and M_2 correspond to the rototranslation matrix that transforms the coordinates from the PRS to the MRS:

$$RT = \begin{pmatrix} R_{3x3} & p_{3x1} \\ f_{1x3} & w_{1x1} \end{pmatrix} = \begin{pmatrix} Rotation & Translation \\ Perspective & Scale \end{pmatrix} \quad (21)$$

This is considered a pure rototranslation, so the perspective vector is null and the scale is considered 1:

$$RT = \begin{pmatrix} R_{3x3} & p_{3x1} \\ 0 & 1 \end{pmatrix} \quad (22)$$

In this way, the test workpiece results can be transformed to the MRS and back to every PRS.

3. Error model and optimization

The kinematic model presented includes 18 of the characteristic 21 errors of three-linear-axes machines. According to many papers on the subject (Schwenke *et al.*, 2008; Sartori and Zhang, 1995), there is a clear correlation between translations, rotations and squareness. The squareness as an independent parameter in the model correlates simultaneously with the constant coefficient of the rotations (a_0) and with the linear coefficient (a_1) of the straightness errors. This fact is reflected in the recommendation, by ISO 230-1, that the first degree coefficient of straightness errors be considered null. This means that only one of these options should be chosen. If the squareness deviations are taken as separate parameters, then the constant term in the rotation must be zero and the straightness should not have a linear term. Our approach is to assimilate each squareness error (ECO, EBO and EAO) in the first degree coefficient (a_1) of the straightness errors (EYX, EZX and EZY) (Kruth *et al.*, 1994), and therefore the rotation terms have no restriction. Each of the errors is considered in the optimization algorithm as a polynomial. The optimization seeks to minimize the mean squared error for all the points supplied. The block diagram of the optimization process is

Figure 3 Rototranslation from MRS system to local PRS

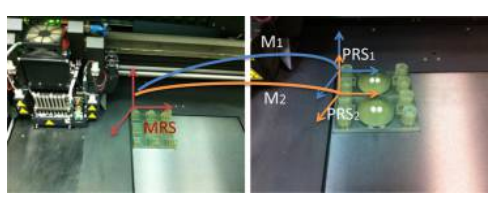

Downloaded by RMIT University At 23:54 09 February 2016 (PT)

shown in Figure 4. The inputs to the system are the actual coordinates of the measured point, the nominal values and the initial values of the polynomial errors. The mean squared error is evaluated iteratively until the convergence criteria are reached. The goal is to find the errors' polynomial coefficients that provide a set of optimized points that are as close as possible to the actual points.

Every iteration, the error of each point is calculated as follows:

$$E_i = \sqrt{(X_{ir} - X_{in})^2 + (Y_{ir} - Y_{in})^2 + (Z_{ir} - Z_{in})^2} \quad (23)$$

Applying the kinematic model, the optimized points are obtained:

$$\begin{pmatrix} X_{ir} \\ Y_{ir} \\ Z_{ir} \end{pmatrix} = f(V) \quad (24)$$

where $f(V)$ is the objective function used during the optimization. V corresponds to the optimization vector, which varies its coefficients at each iteration. In this case, a 1×57 vector containing the coefficients of the Legendre polynomials ordered consecutively is used. The 57 coefficients are placed as follows: three Legendre polynomial coefficients for each of the 18 errors and three printhead offset components.

Many alternatives have been used to approximate each of the error functions, as suggested by different authors, for example Taylor, Chebyshev or B-splines, (Aguado *et al.*, 2012a, 2012b; Dhanish and Shunmugam, 1991; Nakajima, 2006; Philpott and Green, 1995; Sartori and Zhang, 1995). In addition to polynomials, other methods are also suggested such as Bezier curves, Fourier series, wavelets and neural networks (Santolaria *et al.*, 2008). Among the alternatives, Legendre polynomials are used to simulate each parametric error. Each error of translation and rotation is approximated by a linear combination of Legendre polynomials. The degree of the polynomial to be used must be determined first. Degrees of freedom in parametric functions have to be limited because they imply additional computer load in already heavy processes like L-M optimization.

Figure 4 Block diagram of the optimization process

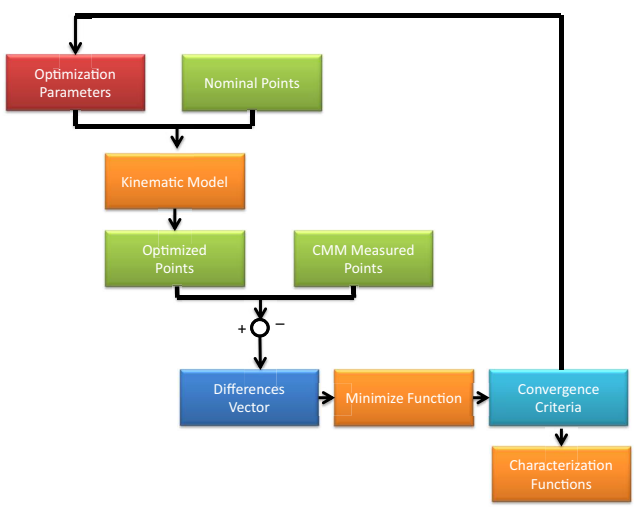

Moreover, as the degree of polynomials increases, the risk of overfitting increases too, which could be worse (Chan *et al.*, 2011; Sartori and Zhang, 1995). Overfitting implies that random errors could be considered to be systematic and therefore the performance of the compensation in further manufacturing could deteriorate. Due to the slow variation of the errors along the axis, it has been decided, based on previous studies (Aguado *et al.*, 2012a, 2012b), to use cubic polynomials. The greater the degree of the polynomial, the lower the obtained residue, but the calculation time and risks of including random noise in the optimization increase. Legendre polynomials have a correlation between coefficients that allows the use of a cubic polynomial with three coefficients instead of four, reducing the computing load. Anyway, the choice of cubic polynomial has to be validated by the obtained results and the correspondence between the forecasted random error and the experimental one.

Generically, a cubic Legendre polynomial is expressed as follows:

$$f(x) = \sum_{i=0}^{3} a_i P^i(x) = a_0 + a_1 x + \frac{1}{2}a_2(3x^2 - 1) + \frac{1}{2}a_3(5x^3 - 3) \quad (25)$$

There are four unknown coefficients in this polynomial that can be reduced to three, assuming that the error is zero when the coordinate x is equal to zero. Therefore correlation between a_0 and a_2 implies that $a_0 = a_2/2$. Substituting a_0, the function can be rewritten as follows:

$$f(x) = a_1 x + a_2\left(\frac{3}{2}x^2\right) + a_3\left(\frac{1}{2}(5x^3 - 3)\right) \quad (26)$$

Applying Legendre polynomials to the errors, each error is replaced by its function:

$$EXX(x) = EXX_1 + EXX_2\left(\frac{3}{2}x^2\right) + EXX_3\left(\frac{1}{2}(5x^3 - 3)\right) \quad (27)$$

where $EXXi$ corresponds to the i Legendre coefficient to be determined by the optimization process, and x corresponds to the axis on which the error depends.

4. Workpiece design and manufacture

As mentioned in the Introduction, the measurement process has to be of high precision, reliable, fast and cost effective. That means that it has to be automatized, minimizing the operator as a source of error and implying lower cost. To achieve high precision, a CMM has been used as the reference measurement device.

Regarding the design of the gauge artefact, conical holes, which have been proven to be very useful in previous works (Santolaria *et al.*, 2010), are proposed as target features whose centres are measured with a self-centring technique provided by the CMM software. The choice of conical sockets is based on the recommendation for the design of kinematic seats in ASME (American National Standards Institute, 2004). We have adapted the Single-Point Articulation Performance Test from *ASME B89.4.22-2004 Methods for Performance*

Downloaded by RMIT University At 23:54 09 February 2016 (PT)

Evaluation of Articulated Arm Coordinate Measuring Machines (American National Standards Institute, 2004) to measure the centre of the cone. Furthermore, polymer materials used in most AM do not have enough rigidity to allow measurement in small boost features (spheres and cylinders). Rather, in this paper, conical holes are suggested as an alternative. The use of inner features allows a denser distribution of points for a certain feature size. It has to be taken into account that undersampling leads to incomplete and inaccurate models that do not detect short-period cyclic errors (Chen *et al.*, 1991). Besides, using smaller features decreases the quantity of shape errors. Moreover, conical sockets can be placed in any surface of the part, just adapting the probing direction and easily ensuring deformation-free probing. Geometrical boss features (external probing), like those used in some other researches (Tong *et al.*, 2008; Moylan *et al.*, 2012), are not so suitable for effective determination of parameters.

The data-sampling process is an original method that, unlike previous ones, does not use a feature identification algorithm (CMM software or custom) for the sampled points. What has been put in place is an adaptation of kinematic socket accommodation that fits a spherical tip probe into a conical socket seat. The CMM self-centring probing strategy sequentially unlocks the two linear degrees of freedom that are orthogonal to the probing direction. The dimensions of the cone are defined for a specific sphere diameter that is so small that shape errors are trivial. Using a 2-mm diameter probing sphere (Figure 5), each measurement provides the coordinates of the centre of the sphere. These coordinates match the intersection of the surface with the centre of the cone. This fitting method has been proven to be fast, accurate and reliable (discrepancies from the nominal position of the cone are absorbed). Anyhow, measurement repeatability studies are carried out to prove these claims in the Results section.

By means of the proposed probing strategy, a density up to 9 points per square centimetre can be achieved due to the small size of the socket, even considering a security margin. As mentioned above, these sockets can be located on any side of the piece and they can be accessed with the appropriate orientation of the probe in the CMM.

The artefact designed for error identification, named the Volumetric Master, is shown in Figure 6. It is a workpiece that covers a volume of 115 × 115 × 50 mm with a total of 233 conical sockets. It consists of a flat base with nine stepped pyramids (P1 to PC). Only the central one, PC, is a complete pyramid. Despite not being a completely homogeneous distribution (Figure 7), the amount of points is considered sufficient in each region.

The piece is designed to increase the density of points at low Z-coordinates, close to the tray, which is normally the zone where the workpieces are manufactured, to avoid support material waste. As shown in Figure 7, the X- and Y-coordinates of the points are equally distributed and the negative values correspond to the Y-coordinate according to MRS in Figure 1. However, this is a design which does not cover the entire operative volume of the machine, but serves to determine a specific zone. To fully cover the volume, it would be necessary to replicate the workpiece four times, with a specific offset at each Z-level required.

Figure 6 Crenelated gauge workpiece

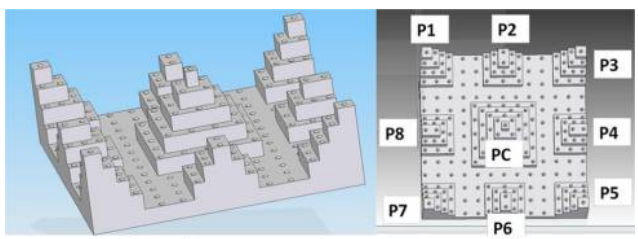

(a) (b)

Notes: (a) 3D view; (b) identification of crenelations

Figure 5 Design of conical sockets

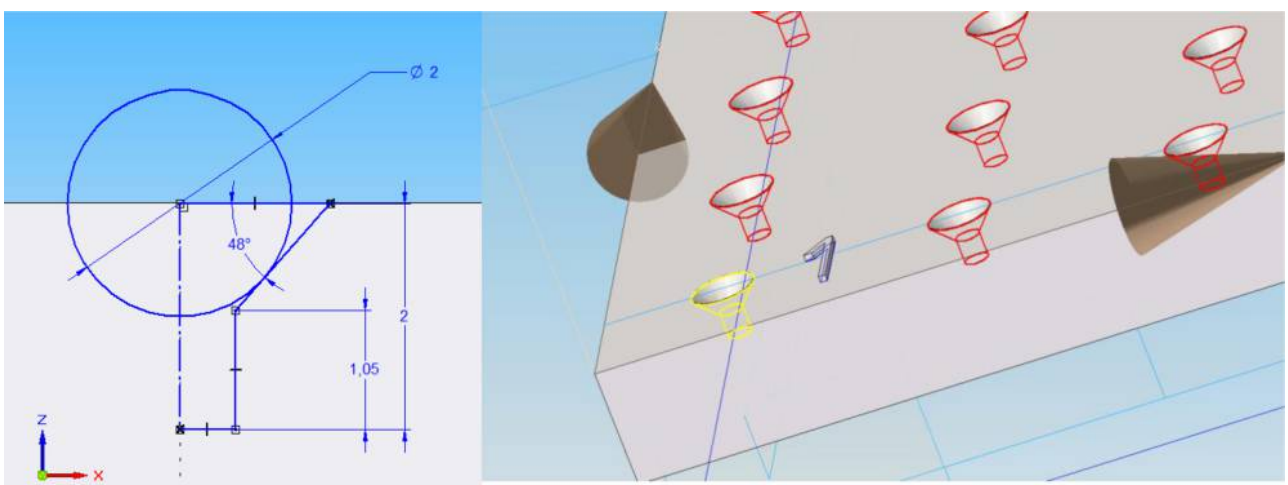

(a) (b)

Notes: (a) Draft of conical socket; (b) sockets in gauge workpiece

Figure 7 Distribution of conical sockets' coordinates

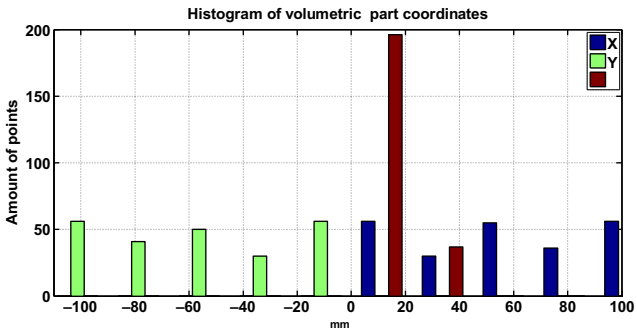

5. Measurement

The measurement process took place in a metrology laboratory in a controlled temperature environment. Three temperature probes (Figure 8) were used to ensure that the results were independent of temperature effects. One temperature probe measures the air, and the other two are placed on the test workpieces, one in contact with and the other isolated from the CMM granite table, for the purpose of studying eventual discrepancies.

A Zeiss PCM 850 CMM with a Vast XT scanning sensor and Calypso software was used as the main measurement equipment. This allows automatic measurements without the operator error factor. For automatic measurement, it is sufficient to establish the workpiece reference system and provide the nominal coordinates of the points for the CMM. The local workpiece reference system is roughly defined by the operator and thereafter it is redefined in automatic mode for each workpiece. Then, the probing tip approaches the nominal coordinates with a security offset in the probing coordinate, for a secure approach, and once there, it automatically reaches the bottom of the socket using the already mentioned self-centring strategy. In the case of the proposed gauge artefact, the probing direction is –Z. Therefore, the probe moves in that direction, unlocking orthogonal degrees of freedom until no further movement is possible. This method is very reliable because discrepancies of some tenths of a millimetre between the actual coordinates and the nominal coordinates of the centre of the cone are no problem for the initial positioning of the probing sphere; however, for larger errors, the nominal coordinates should not be used.

Figure 8 Temperature control system during the measurement

(a) (b)

Notes: (a) Sensors for environmental and material temperature; (b) capturing device

6. Research results

6.1 Repeatability of the measurement system

First of all, the claimed reliability in the use of self-centring probing for conical sockets has to be ensured by running a specific repeatability test. A test to isolate self-centring from other uncertainty sources was performed. A total of 11 measurements were executed on the same socket, and the results are shown in Table II.

As can be seen, the discrepancies between measurements do not reach the 1-μm range in any of the axes in any case, which is the expected result, taking into account the quality of the measurement instrument used.

Unfortunately, the measuring conditions can never be as propitious as in the previous case. So, it is mandatory to perform a larger number of tests with an additional amount of conical sockets. In every case, the workpieces are released and fixed, and the reference system is recalculated for each measurement. The process was deliberately not performed non-stop. In this regard, in some cases, there was an interval of more than 24 hours between measurements. The manufactured workpieces were manufactured in the Objet Eden350V machine with the nominal STL files. The aim of these tests is to evaluate the repeatability of the measuring system, which is a mandatory requirement, prior to error model identification; otherwise, random measurement errors could invalidate the methodology.

The results of performing ten measurements on a gauge artefact with 31 points are shown in Table III. This makes a total of 310 point measurements. The workpiece used in this case is a 320-mm longitudinal gauge artefact oriented according to the X-axis, identical to the one shown in Figure 8.

The same test was done for the workpiece named the Volumetric Master (Figure 6). Four measurements were carried out for each of the 233 points of the gauge artefact at various intervals, over 48 hours with a temperature variation of ± 0.5°C,

Table II Measurement results, single socket repeatability

Iteration	X	Y	Z
1	20.0423	7.4783	−1.0181
2	20.0424	7.4779	−1.0183
3	20.0424	7.4778	−1.0184
4	20.0424	7.4777	−1.0185
5	20.0424	7.4776	−1.0185
6	20.0424	7.4776	−1.0186
7	20.0424	7.4776	−1.0186
8	20.0423	7.4775	−1.0187
9	20.0424	7.4775	−1.0187
10	20.0424	7.4774	−1.0187
11	20.0424	7.4774	−1.0188
Range	0.0001	0.0009	0.0007

Table III Single point measurement repeatability test results: 31-socket workpiece

	SD			Error range		
Error	X	Y	Z	X	Y	Z
Maximum	0.001	0.008	0.001	0.002	0.015	0.003
Mean	0.000	0.003	0.001	0.001	0.008	0.002

Downloaded by RMIT University At 23:54 09 February 2016 (PT)

Downloaded by RMIT University At 23:54 09 February 2016 (PT)

making 233 × 4 = 932 measurements in total, whose results are listed in Table IV.

Analysing these results, we can establish that a mean repeatability of 5 μm in a workpiece that has more than 100 μm of manufacturing error is very positive and will allow the conical socket scanning process to be used as the measurement system. In addition, reproducibility is offered because the workpiece reference system is reallocated on each measurement.

Finally, after testing the measurement process, there is still a test that must be performed to check whether the systematic error is larger than the random error regarding the manufacturing process, which is essential in software compensation, as we have previously stated in the Introduction. The test consists in manufacturing two instances of Volumetric Master workpieces and comparing the result of measuring each point to the corresponding result for the other workpiece. The maximum and mean values after point to point comparison are in Table V.

This test established the maximum performance of the compensation method.

6.2 Error identification results

The first step of the error compensation process is the manufacturing of the Volumetric Master (Figure 6) and its measurement. The results of the measurements of the 233 points indicate a maximum error of 0.228 mm and a mean error of 0.127 mm. After supplying the optimization system with nominal and measured coordinates, the polynomials of the error model are obtained through the iterative L-M optimization process.

Table IV Single point measurement repeatability test results: 233-socket workpiece

	SD			Error range		
Error	**X**	**Y**	**Z**	**X**	**Y**	**Z**
Maximum	0.006	0.007	0.008	0.013	0.013	0.018
Mean	0.002	0.001	0.002	0.003	0.002	0.005

Table V Manufacturing repeatability test results (mm)

Error	**Result**
Maximum	0.059
Mean	0.019

The triangulated mesh of the Volumetric Master workpiece is shown in Figure 9, where a detail of the discrepancies between original and compensated vertices of a particular cone is also shown. STL (3D Systems Inc, 1988) is a file format native to the stereolithography CAD software considered the standard format for 3D printing. The file consists of a list of triangles, each one with three vertices and a normal vector. To perform the compensation, each vertex of the STL file is compensated and the normal vector for each triangle is recalculated (Wang and Chang, 2008).

The Legendre polynomial coefficients obtained in the optimization process are shown in Table VI.

The use of these coefficients makes it possible to obtain error values throughout the axis. The error functions, six for each axis, are represented in Figures 10-12.

Each of the axes has different errors, as expected, as the kinematic model of each is different. As this is a volumetric approach, it is not necessary to find the correspondence of each of the individual errors. This explains why an error may have unrealistic values if its contribution to the final error is small. As

Table VI Legendre polynomial regression coefficients

Error type	**a3**	**a2**	**a1**
EXX	1.14E-07	−3.28E-05	2.51E-03
EXY	−2.30E-09	−1.46E-06	1.09E-04
EXZ	9.50E-09	−1.54E-06	1.53E-04
EAX	−1.37E-05	2.91E-03	1.10E-02
EBX	−3.59E-04	−5.47E-04	−2.38E-04
ECX	2.38E-05	−4.79E-03	−6.00E-03
EYY	1.75E-07	4.64E-05	3.24E-03
EYX	6.27E-08	1.65E-05	4.97E-04
EYZ	2.87E-08	5.42E-06	8.83E-05
EAY	5.70E-04	−1.18E-04	−2.47E-04
EBY	4.46E-04	−7.09E-04	−3.82E-04
ECY	1.74E-03	3.89E-04	5.24E-04
EZZ	−1.26E-06	6.79E-05	−7.77E-04
EZX	−8.66E-07	4.40E-05	−7.04E-04
EZY	−1.30E-07	−7.03E-07	6.32E-04
EAZ	−2.54E-03	1.16E-01	6.40E-03
EBZ	−8.95E-04	6.58E-02	3.26E-03
ECZ	−5.58E-04	4.19E-02	4.78E-03

Figure 9 Error identification

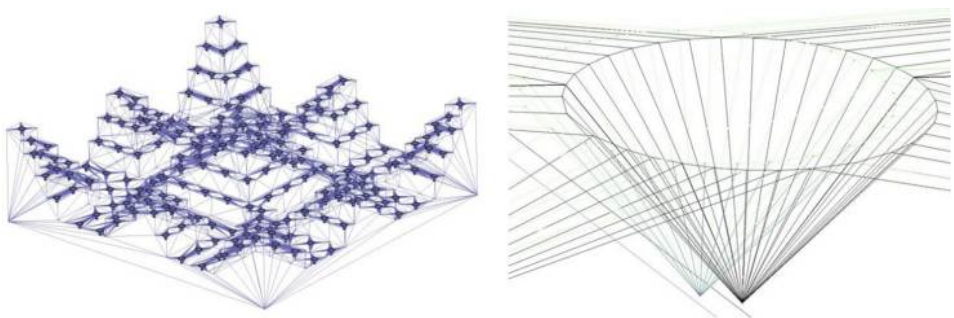

Notes: (a) Original; (b) detail of socket (dark after compensation)

Downloaded by RMIT University At 23:54 09 February 2016 (PT)

Figure 10 X-axis errors

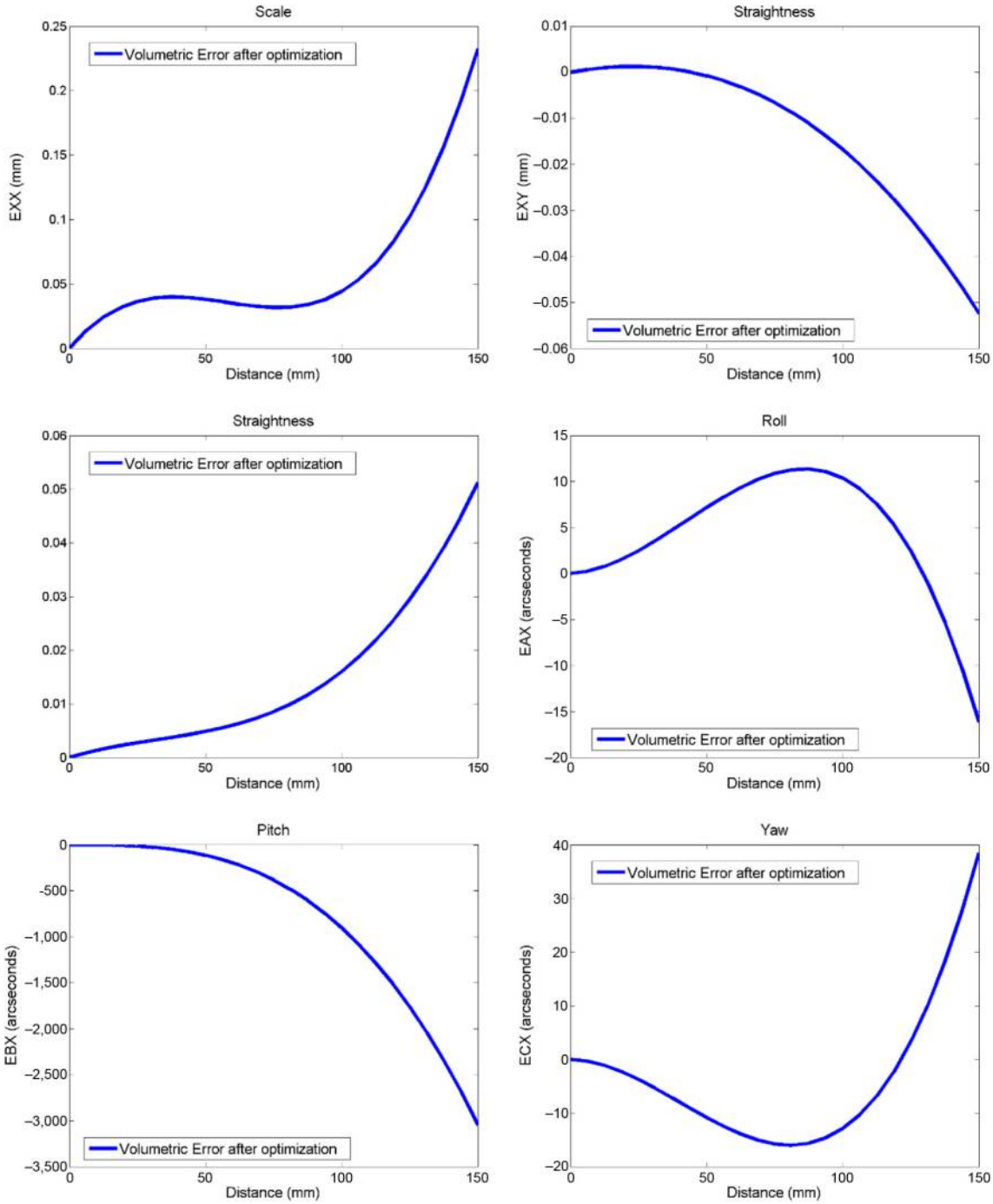

mentioned above, this is the case of EAY error, which, assuming the tool offset is zero, makes no contribution to the final error. Basically, the combined effect of these error functions must be as close as possible to the final error that occurs for each point within the volume.

6.3 Error compensation results

Once the polynomials have been established in the optimization process, the results in terms of final error have to be analysed.

The fitted error (optimized error), which is the ultimate goal of the optimization, is quite close to the measured error, as shown in Figure 13. The maximum and mean discrepancies are 53 and 25 μm, respectively. A complete matching between optimized and measured errors could indicate the absence of random error or insufficiently representative data, which could lead to random error being wrongly assumed to be systematic, which could be worse. The result of subtracting the measured error from the optimized error is the final error, which has to be much lower than the original one and it has also to meet random error

Figure 11 Y-axis errors

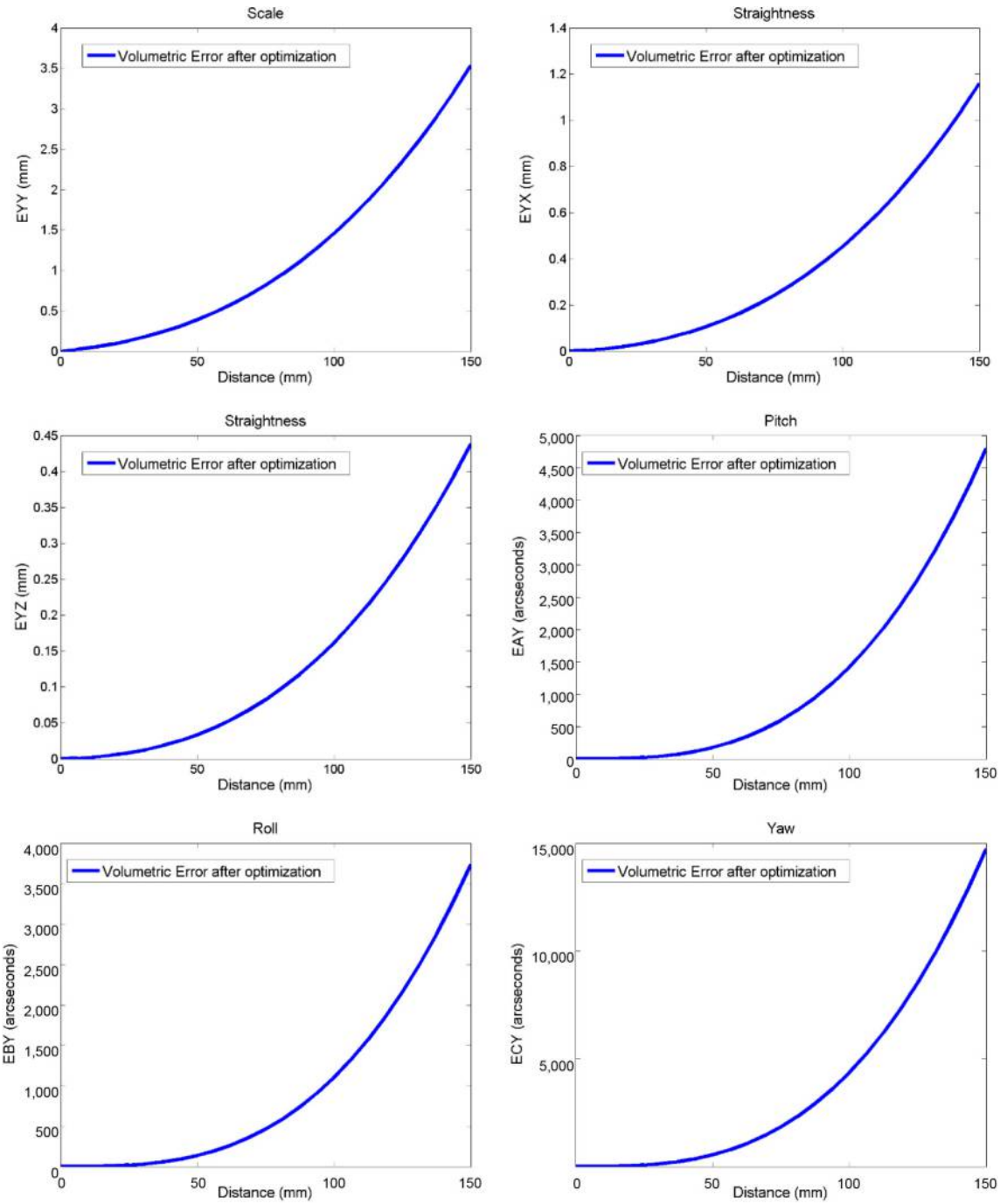

directional characteristics. Although these two requirements are met, the key point for evaluating the results, so far, is to compare the residual error with the results of the manufacturing repeatability. Comparing Tables V and VII, the parametric error identification process can be considered a success.

In Figure 14, it can be appreciated that the directions of the errors are clearly random compared to Figure 13. Also, the modulus has been reduced. This reduction will be discussed in detail along with the actual compensated workpiece error in the Results section. To evaluate the performance of the process, the results in terms of mean error can be used. The mean error drops from the initial value of 127 to 25 μm. That implies a theoretical reduction of up to 81 per cent.

Analysing the histogram of the final error after optimization (Figures 15 and 16), it is important to emphasize that the error modulus has dropped dramatically and that errors per axis are centred to zero as they should be according to the study by Zhu *et al.*, 2010.

To fully appreciate the effects of the optimization, the error has been represented in a 3D graph. The error modulus has been placed as the Z-axis and a colour scale has been used. In Figure 17, the error becomes larger as the distance from the

Downloaded by RMIT University At 23:54 09 February 2016 (PT)

Figure 12 Z-axis errors

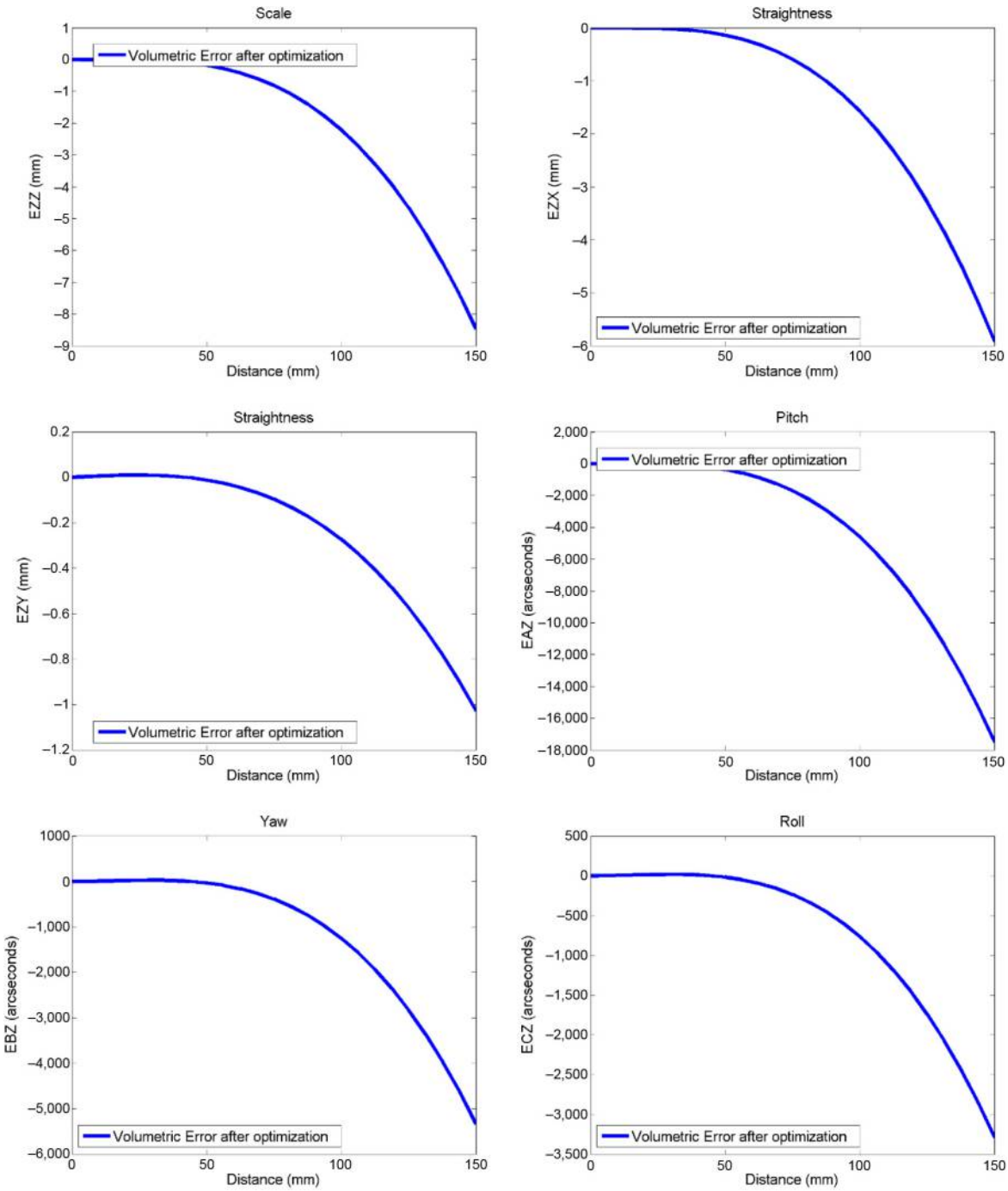

points to the origin increases. However in Figure 18, the error is much smaller and remains at a low level in the whole area.

6.4 Final error results

Once it has been verified that the volumetric compensation leads to great improvement, it is time to manufacture a compensated Volumetric Master workpiece. In this case, the STL has been modified with the compensation of the errors obtained in the optimization process. The original workpiece and the compensated one are shown in Figure 19.

The improvement achieved is shown in Figure 20, where the results in terms of the error modulus are compared, and in Figure 21, in a 3D representation.

The results are summarized in Table VII, where the target value indicates the optimization result. Nevertheless, the figure is illustrative enough, clearly highlighting the similarity between the final error of the compensated workpiece and the forecasted result.

Moreover, the key point is that the results match the manufacturing repeatability. In addition, another important

Downloaded by RMIT University At 23:54 09 February 2016 (PT)

Figure 13 Measured and optimization errors

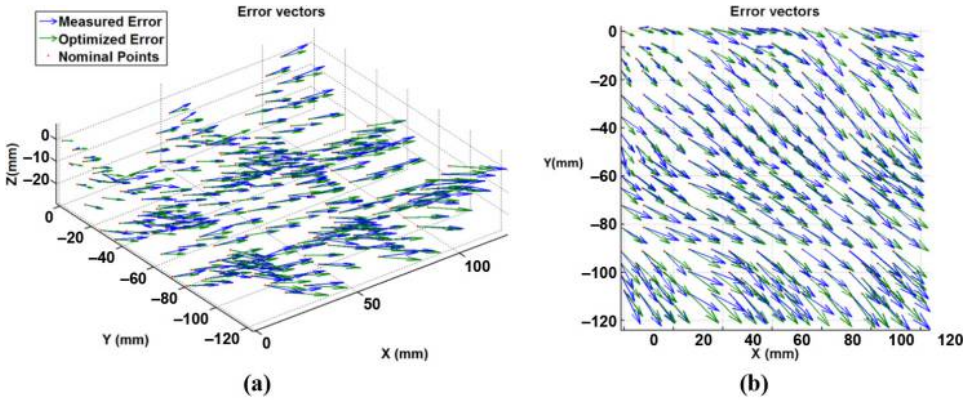

Notes: (a) 3D View; (b) X-Y view

Figure 14 Residual errors

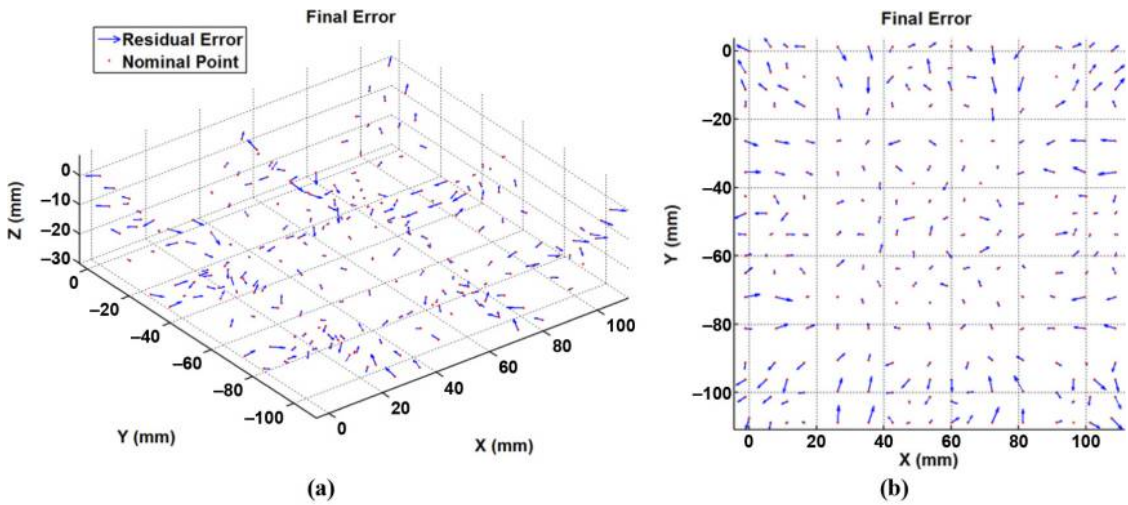

Notes: Scaled x 100; (a) 3D View; (b) X-Y view

Figure 15 Histogram of the final error modulus

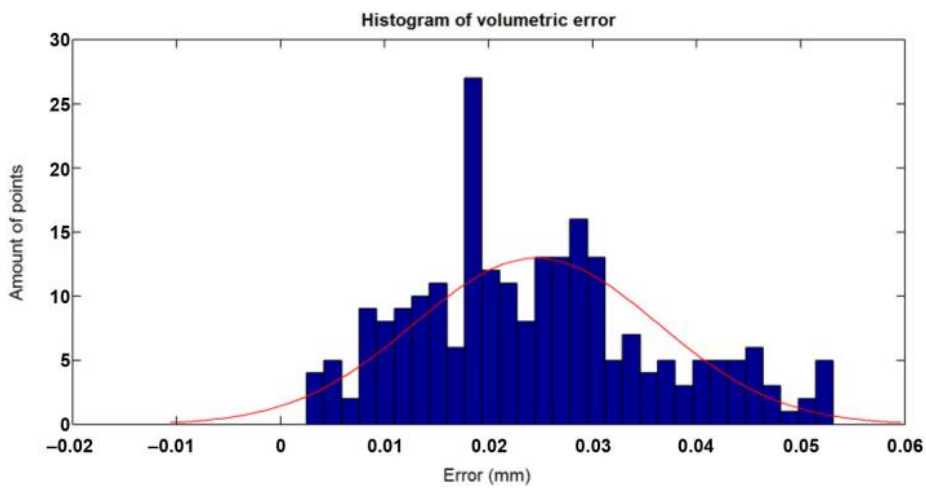

Downloaded by RMIT University At 23:54 09 February 2016 (PT)

Figure 16 Histogram of the final error modulus

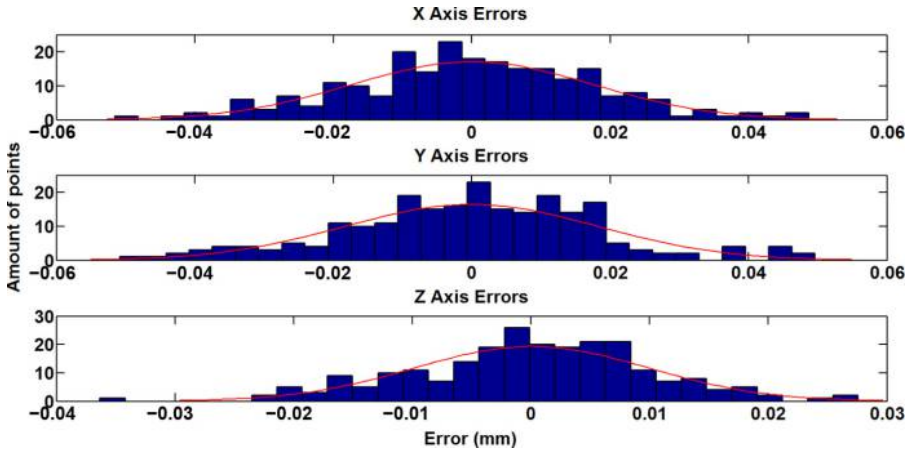

Figure 17 3D error representation before optimization

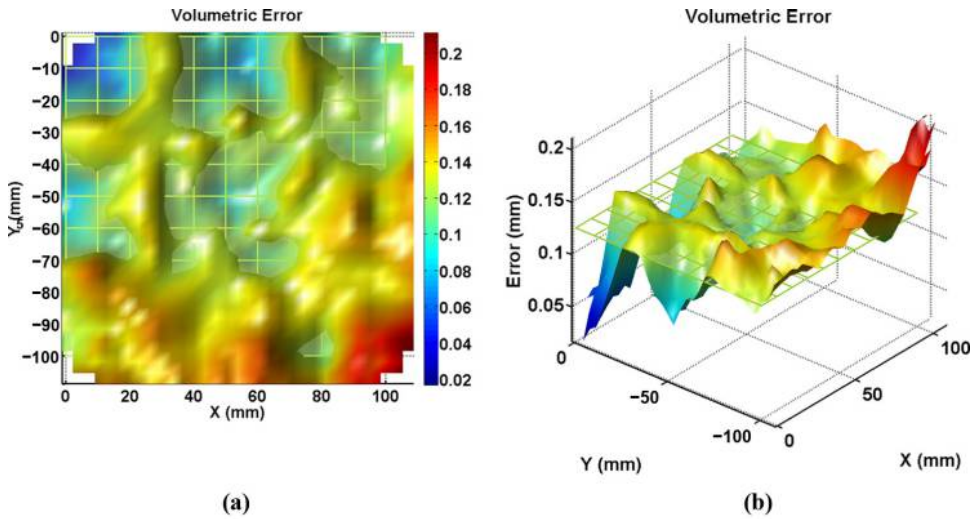

Notes: (a) X-Y view; (b) 3D View

Figure 18 3D error representation after optimization

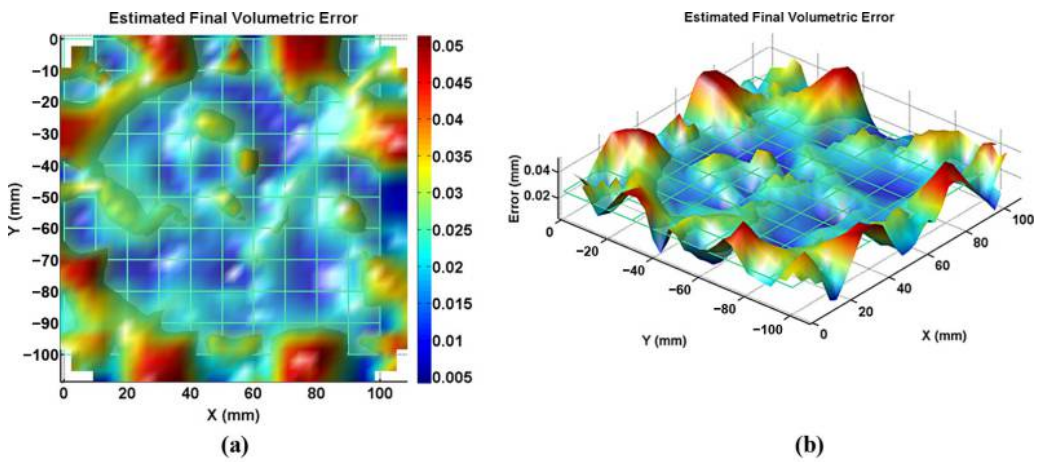

Notes: (a) X-Y view; (b) 3D View

Downloaded by RMIT University At 23:54 09 February 2016 (PT)

Figure 19 Manufactured Volumetric Master workpieces

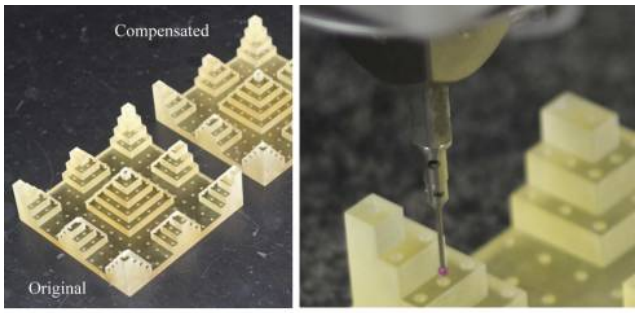

Notes: (a) Both workpieces; (b) probing

issue is that the residues modulus is similar at each point. Therefore, we could conclude that the greatest part of the systematic errors has been compensated and only random error remains in the manufactured workpiece after compensation. These statements can be confirmed clearly in the statistical representations of the error in Figures 22 and 23.

This final error is composed of all the error factors whose contribution is not repeatable and therefore cannot be compensated. Random roughness errors, typical of AM, are included in this remaining error. However, roughness relevance is very process dependant, so in low quality machines, it could invalidate the proposed methodology.

So far, the technique has been verified with conical socket artefacts. However, seeking an actual utility, the same compensation has to be carried out on workpieces with real geometries. An example of the actual features of test workpieces is shown in Figure 24.

Two workpieces were manufactured simultaneously, each in a different placement of the bedplate to test the final rototranslation from PRS to MRS in the kinematic model. Workpiece 1 is placed aligned with WRS and Workpiece 2 has an offset and the same orientation. The design of the workpieces has different geometries to be analysed. The most relevant geometries are the cylinders and the semisphere. The cylinders are named in a clockwise direction from closest to the origin (upper left): 1 to 4 for the outer ones and 5 to 8 for the inner ones. The improvement is generalized in every case, and the results are similar in both workpieces. The results, presented

Figure 20 Comparison of error modulus

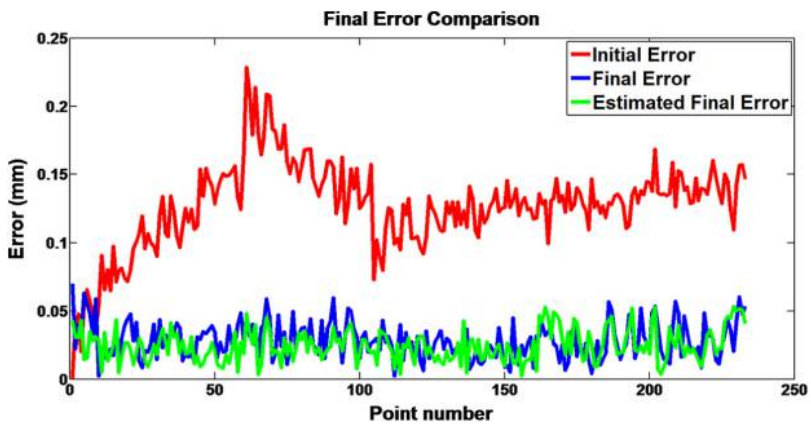

Figure 21 3D final error representation

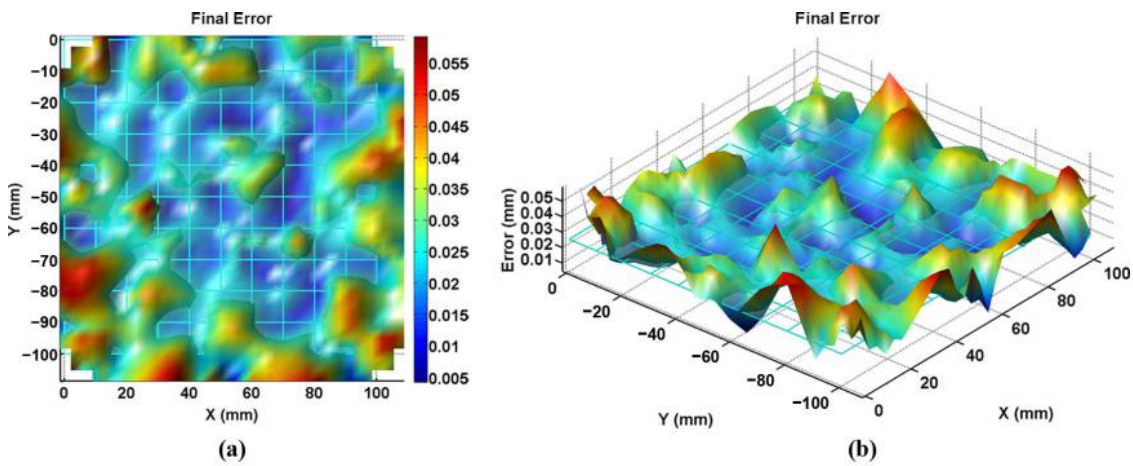

Notes: (a) X-Y view; (b) 3D View

Downloaded by RMIT University At 23:54 09 February 2016 (PT)

Downloaded by RMIT University At 23:54 09 February 2016 (PT)

Table VII Error reduction rates

Error	Initial value	Target	Final value	Improvement rate (%)
Maximum	0.228	0.053	0.070	69.3
Mean	0.127	0.025	0.028	78

in Table VIII, are slightly better for Workpiece 1, but this discrepancy is not significant enough. As Workpiece 2 is farther from the origin, despite the compensation, there could be small discrepancies, because the error reduction is not expected to be equally effective within the whole volume due to the variability in the magnitude of the random error, depending on the location.

The measurement of the cylinder is done by continuous scanning of circles at different Z-levels. CMM software creates a graphical representation, scaling each circle differently. This representation for Cylinder 6 is shown in Figure 25. Although the diameter improvement is important, the improvement in the circle paths of the shape is much more enhanced. This leads to the conclusion that the compensation improvement could be even higher than the one that the numbers reflect.

7. Conclusions

Based on the results, it can be concluded that the use of workpieces as gauge artefacts with conical sockets is a very successful method for placing easy-to-measure points in space. Also, the point density is much higher than when using spheres or cylinders. Related to this, the amount of material required in manufacturing (the main source of cost in 3D printing) is much smaller. Furthermore, the use of unattended scanning minimizes the sources of uncertainty in the measurement process and also reduces its cost.

Once developed the kinematic model, specific to each AM machine, implementing this volumetric compensation technique in that machine type seems very affordable. It may, as well, be used the same design of the gauge artefact. In fact, any AM technology can benefit from this method, as it has been proved that, as long as the error sources are of systematic nature, their combined action can be compensated. The only mandatory requirements are to develop the kinematic model and to obtain a sufficient density of points in the working volume.

One main conclusion is that the results obtained with the application of the method, presented in this paper, could be used by the manufactures to locate and act on the error sources. Additionally, once more by the machine manufacturer, standard calibration procedures could be implemented to detect and correct assembling deficiencies, or to discover the increase of the backlash due to regular working, as part of the supplied software. Moreover, this methodology could also be very useful for machine certification of the machine performance. Regarding the Objet 350 V model in particular, it has been proven that the 3D printer meets the

Figure 22 Final error modulus histogram

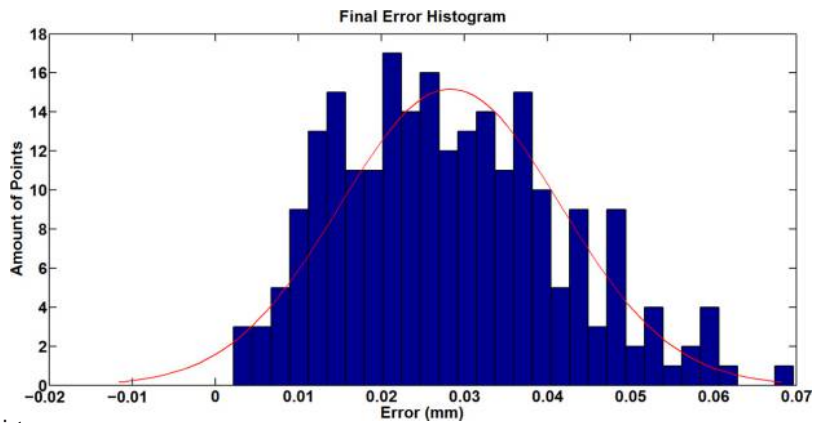

Figure 23 Final axis error histogram

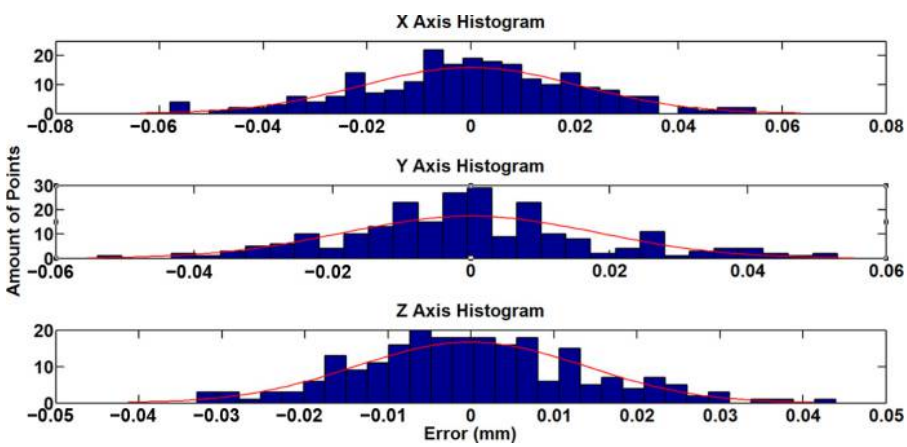

Figure 24 Test workpieces

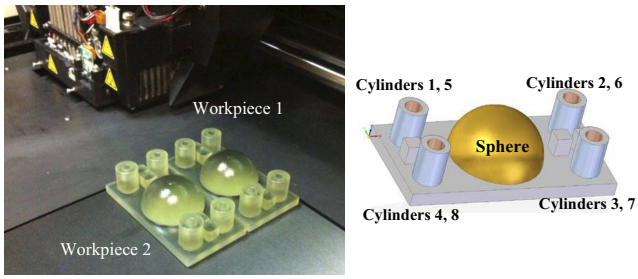

Notes: (a) Manufactured workpieces on tray; (b) identification of characteristics

manufacturer's specifications. However, with this method, the performance is significantly increased, with an improvement of 70 per cent regarding the single point maximum error for the evaluated volume.

A relevant advantage of this technique is that, acting on the source CAD files instead of doing it on the machine implies that any final user can increase the precision of the machine without requiring the support of the manufacturer, and enlarging, this way, the productive life of the machine, dynamically compensating the increasing lack of precision, typically associated to the elapsed working hours.

Concerning future work, it has to be taken into account that the method has been developed on a single type of machine and using the same material in all the experiments. Therefore, additional experimentations with different additive materials have to be carried out to identify the specific contribution of the material to the final error. Finally, based on the nature of the geometric errors, such high density of points in the volume may be avoided, thus resulting in a more efficient measurement

Table VIII Initial distances and after compensation for both workpieces (mm)

Characteristic	Nominal value	Original error	Error: Workpiece 1	Error: Workpiece 2
Sphere /Ø	48.000	0.176	0.080	0.100
Cylinder 1 /Ø	15.000	0.155	0.046	0.081
Cylinder 2 /Ø	15.000	0.148	0.052	0.047
Cylinder 3 /Ø	15.000	0.165	0.061	0.067
Cylinder 4 /Ø	15.000	0.174	0.035	0.081
Cylinder 5 /Ø	9.000	−0.216	0.033	0.061
Cylinder 6 /Ø	9.000	−0.236	0.087	0.094
Cylinder 7 /Ø	9.000	−0.189	0.005	0.050
Cylinder 8 /Ø	9.000	−0.186	0.024	0.037

Figure 25 Shape analysis for a cylinder

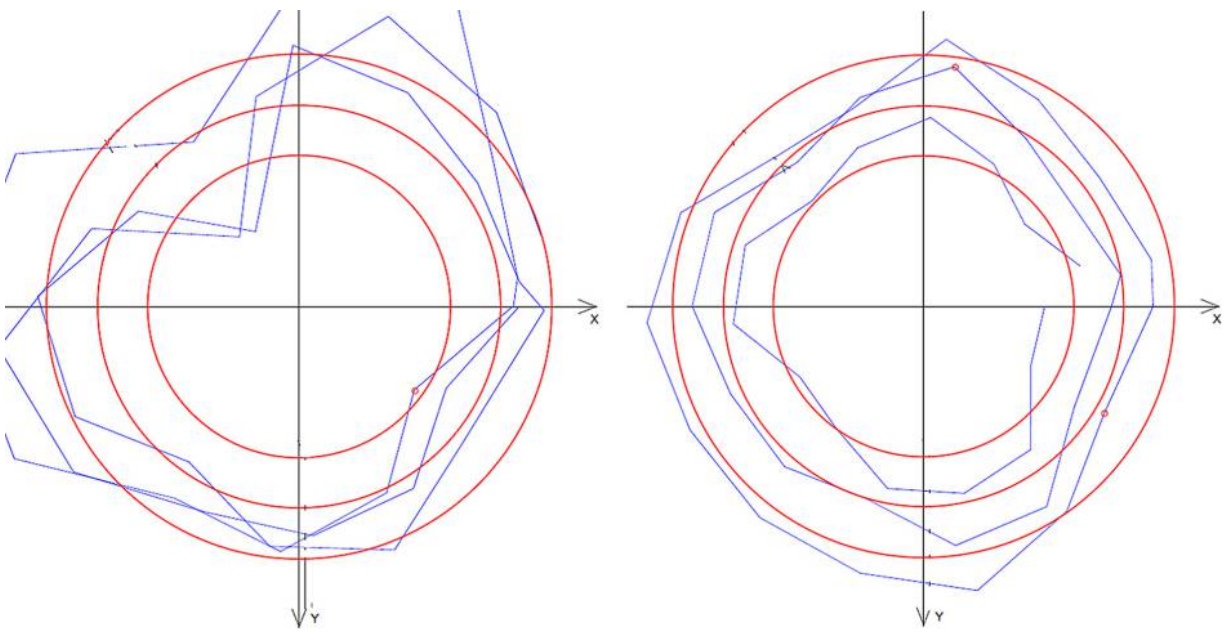

Notes: (a) Before compensation; (b) after compensation

Downloaded by RMIT University At 23:54 09 February 2016 (PT)

process. Hence, specific testing to define the required sample rate has to be performed for each machine design.

References

Aguado, S., Samper, D., Santolaria, J. and Aguilar, J.J. (2012a), "Identification strategy of error parameter in volumetric error compensation of machine tool based on laser tracker measurements", *International Journal of Machine Tools and Manufacture*, Vol. 53 No. 1, pp. 160-169, available at: http://linkinghub.elsevier.com/retrieve/pii/S0890695511002173 (accessed 8 August 2013).

Aguado, S., Samper, D., Santolaria, J. and Aguilar, J.J. (2012b), "Towards an effective identification strategy in volumetric error compensation of machine tools", *Measurement Science and Technology*, Vol. 23 No. 6, p. 65003, available at: http://stacks.iop.org/0957-0233/23/i=6/a=065003?key=crossref.af226b7e7a4730a4984976913233e13c (accessed 2 May 2014).

American National Standards Institute (2004), *ANSI/ASME B89.4.22-2004: Method for Performance Evaluation of Coordinate Measuring Machines*, American National Standards Institute.

Campbell, I., Bourell, D. and Gibson, I. (2012), "Additive manufacturing: rapid prototyping comes of age", *Rapid Prototyping Journal*, Vol. 18 No. 4, pp. 255-258, available at: www.emeraldinsight.com/10.1108/13552541211231563 (accessed 30 March 2014).

Chan, K.Y., Kwongb, C.K., Dillona, T.S. and Tsimb, Y.C. (2011), "Reducing overfitting in manufacturing process modeling using a backward elimination based genetic programming", *Applied Soft Computing*, Vol. 11 No. 2, pp. 1648-1656, available at: http://linkinghub.elsevier.com/retrieve/pii/S1568494610001018 (accessed 18 August 2013).

Chen, J.S., Yuan, J.X., Ni, J. and Wu, S.M. (1991), "Real-time compensation of time-variant volumetric error on a machining center", American Society of Mechanical Engineers, Production Engineering Division (Publication) PED, ASME, pp. 241-253, available at: www.scopus.com/inward/record.url?eid=2-s2.0-0026369608&partnerID=tZOtx3y1

Choi, J.-Y., Choi, J.H., Kim, N.K., Kim, Y., Lee, J.K., Kim, M.K., Lee, J.H. and Kim, M.J. (2002), "Analysis of errors in medical rapid prototyping models", *International Journal of Oral and Maxillofacial Surgery*, Vol. 31 No. 1, pp. 23-32.

3D Systems Inc (1988), *Stereolithography Interface Specification*, 3D Systems Inc.

Dhanish, P.B. and Shunmugam, M.S. (1991), "An algorithm for form error evaluation – using the theory of discrete and linear Chebyshev approximation", *Computer Methods in Applied Mechanics and Engineering*, Vol. 92 No. 3, pp. 309-324.

Dimitrov, D., van Wijck, W., Schreve, K. and de Beer, N. (2006), "Investigating the achievable accuracy of three dimensional printing", *Rapid Prototyping Journal*, Vol. 12 No. 1, pp. 42-52, available at: www.emeraldinsight.com/10.1108/13552540610637264

Hanumaiah, N. and Ravi, B. (2007), "Rapid tooling form accuracy estimation using region elimination adaptive search based sampling technique", *Rapid Prototyping Journal*, Vol. 13 No. 3, pp. 182-190, available at: www.emeraldinsight.com/journals.htm?articleid=1610443&show=abstract (accessed 30 March 2014).

Hocken, R., Simpson, J.A., Borchardt, B., Lazar, J., Reeve, C and Stein, P. (1977), "Three dimensional metrology", *CIRP Annals*, Vol. 26 No. 2, pp. 403-408, available at: http://scholar.google.com/scholar?hl=en&btnG=Search&q=intitle:Three+Dimensional+Metrology#0 (accessed 29 April 2014).

Jung, J., Choi, J. and Lee, S. (2006), "Machining accuracy enhancement by compensating for volumetric errors of a machine tool and on-machine measurement", *Journal of Materials Processing Technology*, Vol. 174 Nos 1/3, pp. 56-66, available at: http://linkinghub.elsevier.com/retrieve/pii/S0924013605003249 (accessed 15 August 2013).

Kruth, J.P., Vanherck, P. and De Jonge, L. (1994), "Self-calibration method and software error correction for three-dimensional coordinate measuring machines using artefact measurements", *Measurement*, Vol. 14 No. 2, pp. 157-167, available at: www.sciencedirect.com/science/article/pii/0263224194900248 (accessed 12 April 2014).

Levenberg, K. (1944), "A method for the solution of certain problems in least squares", *Quarterly of Applied Mathematics*, Vol. 2 No. 1, pp. 164-168.

Liu, W., Li, L. and Kochhar, A.K. (1998a), "A method for assessing geometrical errors in layered manufacturing: Part 1: error interaction and transfer mechanisms", *The International Journal of Advanced Manufacturing Technology*, Vol. 14 No. 9, pp. 637-643, available at: http://dx.doi.org/10.1007/BF01192283 (accessed 16 April 2014).

Liu, W., Li, L. and Kochhar, A.K. (1998b), "A method for assessing geometrical errors in layered manufacturing. Part 2: mathematical modelling and numerical evaluation", *The International Journal of Advanced Manufacturing Technology*, Vol. 14 No. 9, pp. 644-650, available at: http://dx.doi.org/10.1007/BF01192284 (accessed 16 April 2014).

Marquardt, D.W. (1963), "An algorithm for least-squares estimation of nonlinear parameters", *Journal of the Society for Industrial & Applied Mathematics*, Vol. 11 No. 2, pp. 431-441.

Moylan, S., Cooke, A., Jurrens, K., Slotwinski, J. and Donmez, M.A. (2012), "A review of test artifacts for additive manufacturing", available at: http://nvlpubs.nist.gov/nistpubs/ir/2012/NIST.IR.7858.pdf (accessed 30 March 2014).

Moylan, S., Slotwinski, J., Cooke, A.L., Jurrens, K.K., Donmez, M.A. (2012), "Proposal for a standardized test artifact for additive manufacturing machines and processes", *Proceedings of the 2012 Annual International Solid Freeform Fabrication Symposium, Austin, TX*, pp. 6-8.

Nakajima, M. (2006), "Note on Chebyshev regression", UIUC, Jan.

Philpott, M.L. and Green, P.A. (1995), "An error compensation strategy for replication by rapid prototyping", *Journal of Engineering for Industry*, Vol. 117 No. 3, p. 423, available at: http://dx.doi.org/10.1115/1.2804350 (accessed 24 April 2014).

Santolaria, J., Aguilar, J.-J., Yagüe, J.-A. and Pastor, J. (2008), "Kinematic parameter estimation technique for calibration

Downloaded by RMIT University At 23:54 09 February 2016 (PT)

and repeatability improvement of articulated arm coordinate measuring machines", *Precision Engineering*, Vol. 32 No. 4, pp. 251-268, available at: http://linkinghub.elsevier.com/retrieve/pii/S0141635907001146 (accessed 19 March 2014).

Santolaria, J., Brau, A., Velázquez, J. and Aguilar, J.J. (2010), "A self-centering active probing technique for kinematic parameter identification and verification of articulated arm coordinate measuring machines", *Measurement Science and Technology*, Vol. 21 No. 5, p. 055101, available at: http://stacks.iop.org/0957-0233/21/i=5/a=055101?key=crossref.683b5a128620c95d311c88cfb0ea139b (accessed 10 October 2013).

Sartori, S. and Zhang, G. (1995), "Geometric error measurement and compensation of machines", *CIRP Annals – Manufacturing Technology*, Vol. 44 No. 2, pp. 599-609, available at: www.sciencedirect.com/science/article/pii/S0007850607605071 (accessed 19 March 2014).

Schwenke, H., Knappb, W., Haitjemac, H., Weckenmannd, A., Schmitte, R. and Delbressinef, F. (2008), "Geometric error measurement and compensation of machines – an update", *CIRP Annals – Manufacturing Technology*, Vol. 57 No. 2, pp. 660-675, available at: http://linkinghub.elsevier.com/retrieve/pii/S0007850608001960 (accessed 19 March 2014).

Tong, K., Joshi, S. and Lehtihet, E. (2008), "Error compensation for fused deposition modeling (FDM) machine by correcting slice files", *Rapid Prototyping Journal*, Vol. 14 No. 1, pp. 4-14, available at: www.emeraldinsight.com/10.1108/13552540810841517 (accessed 18 August 2013).

Tong, K., Lehtihet, E.A. and Joshi, S. (2004), "Software compensation of rapid prototyping machines", *Precision Engineering*, Vol. 28 No. 3, pp. 280-292, available at: www.sciencedirect.com/science/article/pii/S0141635903001594 (accessed 29 March 2014).

Wang, C.-S. and Chang, T.-R. (2008), "Re-triangulation in STL meshes for rapid prototyping and manufacture", *The International Journal of Advanced Manufacturing Technology*, Vol. 37 Nos 7/8, pp. 770-781.

Wang, S.-M., Liu, Y.-L. and Kang, Y. (2002), "An efficient error compensation system for CNC multi-axis machines", *International Journal of Machine Tools and Manufacture*, Vol. 42 No. 11, pp. 1235-1245, available at: http://linkinghub.elsevier.com/retrieve/pii/S0890695502000536 (accessed 23 March 2014).

Wilhelm, R.G., Srinivasan, N., Farabaugh, F. and Hocken, R. (1997), "Part form errors predicted from machine tool performance measurements", *CIRP Annals – Manufacturing Technology*, Vol. 46 No. 1, pp. 471–474, available at: www.sciencedirect.com/science/article/pii/S0007850607608683 (accessed 29 March 2014).

Xu, F., Wong, Y.S. and Loh, H.T. (2000), "Toward Generic Models for Comparative Rapid Prototyping and Manufacturing", *Journal of Manufacturing Systems*, Vol. 19 No. 5, pp. 283-296.

Yan, X. and Gu, P. (1996), "A review of rapid prototyping technologies and systems", *Computer-Aided Design*, Vol. 28 No. 4, pp. 307-318, available at: www.sciencedirect.com/science/article/pii/0010448595000356 (accessed 25 March 2014).

Zhu, W., Wang, Z. and Yamazaki, K. (2010), "Machine tool component error extraction and error compensation by incorporating statistical analysis", *International Journal of Machine Tools and Manufacture*, Vol. 50 No. 9, pp. 798-806, available at: http://linkinghub.elsevier.com/retrieve/pii/S0890695510001021 (accessed 3 August 2013).

Corresponding author

Carlos Cajal can be contacted at: ccajal@unizar.es

Downloaded by RMIT University At 23:54 09 February 2016 (PT)

For instructions on how to order reprints of this article, please visit our website:
www.emeraldgrouppublishing.com/licensing/reprints.htm
Or contact us for further details: **permissions@emeraldinsight.com**